CLIC Detector and Physics Project

Eva Sicking (CERN)
on behalf of the CLICdp collaboration

CLIC workshop
January 28, 2015

CLICdp: CLIC Detector and Physics

- Collaboration for CLIC-specific detector R&D
  → Physics prospects through simulation studies
  → Detector optimisation and R&D for CLIC
- Strong links to ILC detector concepts, CALICE, FCAL
- Details at http://clicdp.web.cern.ch/

- "Light-weight" collaboration structure
- 25 institutes, 5 new institutes in 2014
- New members are welcome to join!

CLIC physics program

- High luminosity over wide range of $\sqrt{s}$
  $\rightarrow$ staged construction
- CLIC energy stages defined by physics
  $\rightarrow$ adapt to discoveries at LHC

- Currently proposed scenario
  - $\sqrt{s}$=360 GeV, 500 fb^{-1}
    - SM Higgs physics including total width measurement
    - Top threshold scan
  - $\sqrt{s}$=1.4 TeV, 1.5 ab^{-1}
    - New physics
    - $t\bar{t}H$, Higgs self coupling
    - Rare Higgs decays
  - $\sqrt{s}$=3 TeV, 2 ab^{-1}
    - New physics
    - Higgs self coupling
    - Rare Higgs decays

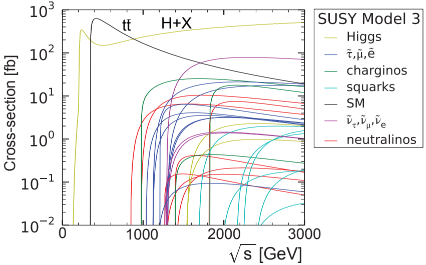

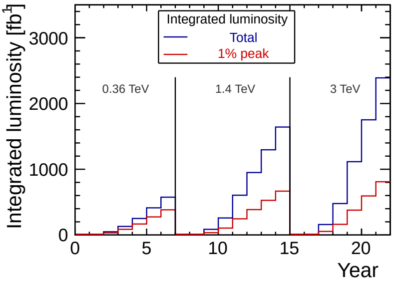

CLIC physics program

→Talk by M. Thomson (Friday)

- High luminosity over wide range of $\sqrt{s}$
  → staged construction
- CLIC energy stages defined by physics
  → adapt to discoveries at LHC

- Currently proposed scenario
  - $\sqrt{s}$=360 GeV, 500 fb^{-1}
    - SM Higgs physics including total width measurement
    - Top threshold scan
  - $\sqrt{s}$=1.4 TeV, 1.5 ab^{-1}
    - New physics
    - $t\bar{t}H$, Higgs self coupling
    - Rare Higgs decays
  - $\sqrt{s}$=3 TeV, 2 ab^{-1}
    - New physics
    - Higgs self coupling
    - Rare Higgs decays

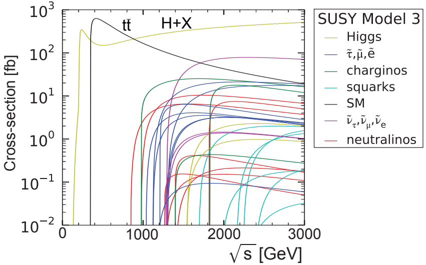

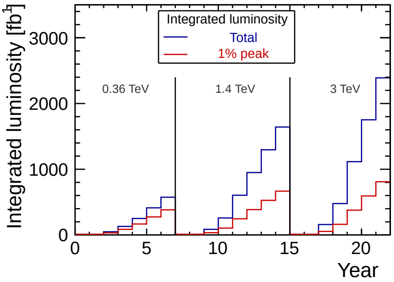

Higgs physics at CLIC (1)

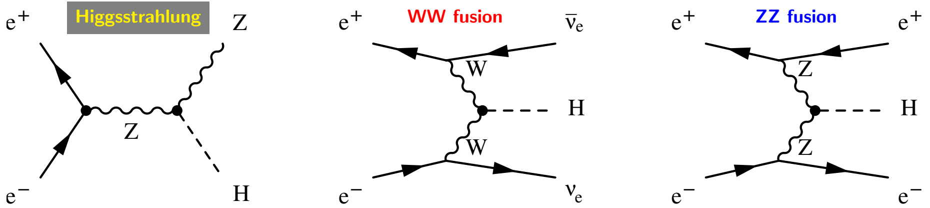

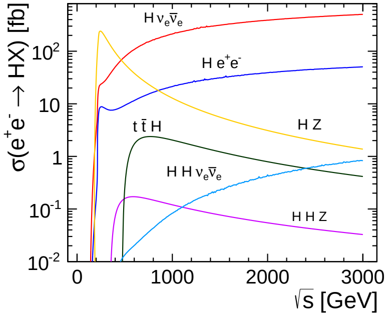

	350 GeV	1.4 TeV	3 TeV
L_{int}	500 fb^{-1}	1.5 ab^{-1}	2 ab^{-1}
# ZH events	68 000	20 000	11 000
# $H\nu_e\bar{\nu}_e$ events	17 000	370 000	830 000
# He^+e^- events	3 700	37 000	84 000

- Large samples of Higgs bosons achievable at CLIC without beam polarisation
- 80 % e^- polarisation foreseen at CLIC
  $\rightarrow$ 12 % more HZ and He^+e^- events
  $\rightarrow$ 80 % more $H\nu_e\bar{\nu}_e$ events

Higgs physics at CLIC (2)

Top Yukawa coupling

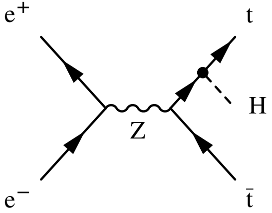

Trilinear self coupling

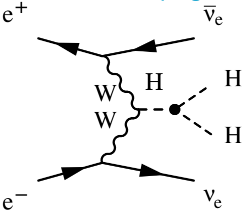

Quartic coupling

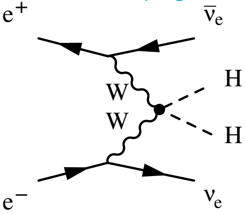

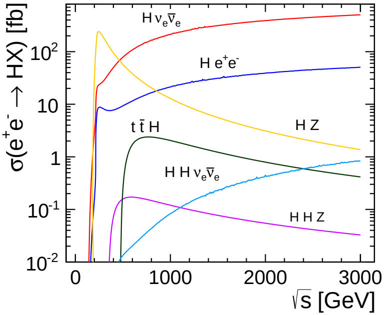

	1.4 TeV	3 TeV
L_{int}	1.5 ab^{-1}	2 ab^{-1}
# $t\bar{t}H$ events	2400	1400
# $HH\nu_e\bar{\nu}_e$ events	225	1 200

- High energies and luminosities needed to access rare Higgs production processes

Higgsstrahlung at $\sqrt{s} = 350$ GeV

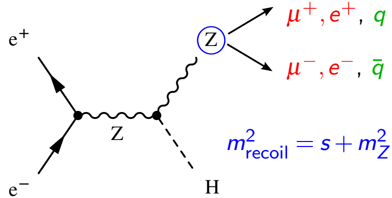

$$m^2_{\text{recoil}} = s + m^2_Z - 2E_z\sqrt{s}$$

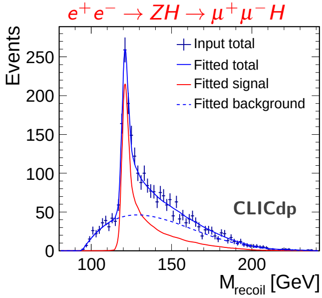

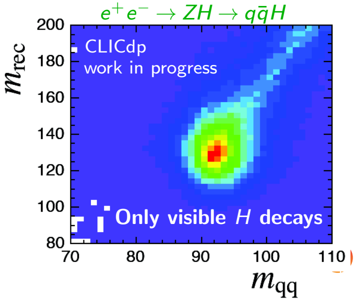

- Measure HZ events from Z recoil mass
- Includes invisible Higgs decays
- Measurement of g_{HZZ} coupling
- $Z \to e^+e^- / \mu^+\mu^-$ decay
  - $\text{BR}(Z \to \mu\mu/ee) \approx 7\,\%$
  - Fully model independent
  - $\Delta\sigma_{HZ}/\sigma_{HZ} \approx 4.2\,\% \to \Delta(g_{HZZ})/g_{HZZ} \approx 2.1\,\%$
- $Z \to q\bar{q}$ decay
  - $\text{BR}(Z \to q\bar{q}) \approx 70\,\%$
  - Challenge: $Z \to q\bar{q}$ reconstruction may depend on H decay mode
  - $\Delta\sigma_{HZ}/\sigma_{HZ} \approx 1.8\,\% \to \Delta(g_{HZZ})/g_{HZZ} \approx 0.9\,\%$

Results from full Geant4 detector simulations including backgrounds

Channel	Measurement	Observable	Statistical precision: 350 GeV, 500 fb^{-1}	1.4 TeV, 1.5 ab^{-1}	3.0 TeV, 2.0 ab^{-1}
ZH	Recoil mass distribution	m_H	120 MeV	–	–
ZH	$\sigma(HZ) \times \text{BR}(H \to \text{invisible})$	Γ_{inv}	0.6%	–	–
ZH	$H \to b\bar{b}$ mass distribution	m_H	tbd	–	–
$H\nu_e\bar{\nu}_e$	$H \to b\bar{b}$ mass distribution	m_H	–	40 MeV*	33 MeV*
ZH	$\sigma(HZ) \times \text{BR}(Z \to l^+l^-)$	g^2_{HZZ}	4.2%	–	–
ZH	$\sigma(HZ) \times \text{BR}(Z \to q\bar{q})$	g^2_{HZZ}	1.8%	–	–
ZH	$\sigma(HZ) \times \text{BR}(H \to b\bar{b})$	$g^2_{HZZ}g^2_{Hbb}/\Gamma_H$	1%†	–	–
ZH	$\sigma(HZ) \times \text{BR}(H \to c\bar{c})$	$g^2_{HZZ}g^2_{Hcc}/\Gamma_H$	5%†	–	–
ZH	$\sigma(HZ) \times \text{BR}(H \to gg)$		6%†	–	–
ZH	$\sigma(HZ) \times \text{BR}(H \to \tau^+\tau^-)$	$g^2_{HZZ}g^2_{H\tau\tau}/\Gamma_H$	6.2%	–	–
ZH	$\sigma(HZ) \times \text{BR}(H \to WW^*)$	$g^2_{HZZ}g^2_{HWW}/\Gamma_H$	2%†	–	–
ZH	$\sigma(HZ) \times \text{BR}(H \to ZZ^*)$	$g^2_{HZZ}g^2_{HZZ}/\Gamma_H$	tbd	–	–
$H\nu_e\bar{\nu}_e$	$\sigma(H\nu_e\bar{\nu}_e) \times \text{BR}(H \to b\bar{b})$	$g^2_{HWW}g^2_{Hbb}/\Gamma_H$	3%†	0.3%	0.2%
$H\nu_e\bar{\nu}_e$	$\sigma(H\nu_e\bar{\nu}_e) \times \text{BR}(H \to c\bar{c})$	$g^2_{HWW}g^2_{Hcc}/\Gamma_H$	–	2.9%	2.7%
$H\nu_e\bar{\nu}_e$	$\sigma(H\nu_e\bar{\nu}_e) \times \text{BR}(H \to gg)$		–	1.8%	1.8%
$H\nu_e\bar{\nu}_e$	$\sigma(H\nu_e\bar{\nu}_e) \times \text{BR}(H \to \tau^+\tau^-)$	$g^2_{HWW}g^2_{H\tau\tau}/\Gamma_H$	–	4.2%	tbd
$H\nu_e\bar{\nu}_e$	$\sigma(H\nu_e\bar{\nu}_e) \times \text{BR}(H \to \mu^+\mu^-)$	$g^2_{HWW}g^2_{H\mu\mu}/\Gamma_H$	–	38%	16%
$H\nu_e\bar{\nu}_e$	$\sigma(H\nu_e\bar{\nu}_e) \times \text{BR}(H \to \gamma\gamma)$		–	15%	tbd
$H\nu_e\bar{\nu}_e$	$\sigma(H\nu_e\bar{\nu}_e) \times \text{BR}(H \to Z\gamma)$		–	42%	tbd
$H\nu_e\bar{\nu}_e$	$\sigma(H\nu_e\bar{\nu}_e) \times \text{BR}(H \to WW^*)$	g^4_{HWW}/Γ_H	tbd	1.4%	0.9%
$H\nu_e\bar{\nu}_e$	$\sigma(H\nu_e\bar{\nu}_e) \times \text{BR}(H \to ZZ^*)$	$g^2_{HWW}g^2_{HZZ}/\Gamma_H$	–	3%†	2%†
Hee	$\sigma(Hee) \times \text{BR}(H \to b\bar{b})$	$g^2_{HZZ}g^2_{Hbb}/\Gamma_H$	–	1%†	0.7%†
$t\bar{t}H$	$\sigma(t\bar{t}H) \times \text{BR}(H \to b\bar{b})$	$g^2_{Ht\bar{t}}g^2_{Hbb}/\Gamma_H$	–	8%	tbd
$HH\nu_e\bar{\nu}_e$	$\sigma(HH\nu_e\bar{\nu}_e)$	g_{HHWW}	–	7%*	3%*
$HH\nu_e\bar{\nu}_e$	$\sigma(HH\nu_e\bar{\nu}_e)$	λ	–	32%	16%
$HH\nu_e\bar{\nu}_e$	with -80% e^- polarisation	λ	–	24%	12%

Results without beam polarisation

†: estimated, *: preliminary

→Physics and analysis session (Thursday)

Results from full Geant4 detector simulations including backgrounds

Channel	Measurement	Observable	Statistical precision		
			350 GeV 500 fb^{-1}	1.4 TeV 1.5 ab^{-1}	3.0 TeV 2.0 ab^{-1}
ZH	Recoil mass distribution	m_H	120 MeV	–	–
ZH	$\sigma(HZ) \times \mathrm{BR}(H \to \text{invisible})$	Γ_{inv}	0.6%	–	–
ZH	$H \to b\bar{b}$ mass distribution	m_H	tbd	–	–
$H\nu_e\bar{\nu}_e$	$H \to b\bar{b}$ mass distribution	m_H	–	40 MeV*	33 MeV*
ZH	$\sigma(HZ) \times \mathrm{BR}(Z \to l^+l^-)$	g^2_{HZZ}	4.2%	–	–
ZH	$\sigma(HZ) \times \mathrm{BR}(Z \to q\bar{q})$	g^2_{HZZ}	1.8%	–	–
ZH	$\sigma(HZ) \times \mathrm{BR}(H \to b\bar{b})$	$g^2_{HZZ}g^2_{Hbb}/\Gamma_H$	1%†	–	–
ZH	$\sigma(HZ) \times \mathrm{BR}(H \to c\bar{c})$	$g^2_{HZZ}g^2_{Hcc}/\Gamma_H$	5%†	–	–
ZH	$\sigma(HZ) \times \mathrm{BR}(H \to gg)$		6%†	–	–
ZH	$\sigma(HZ) \times \mathrm{BR}(H \to \tau^+\tau^-)$	$g^2_{HZZ}g^2_{H\tau\tau}/\Gamma_H$	6.2%	–	–
ZH	$\sigma(HZ) \times \mathrm{BR}(H \to WW^*)$	$g^2_{HZZ}g^2_{HWW}/\Gamma_H$	2%†	–	–
ZH	$\sigma(HZ) \times \mathrm{BR}(H \to ZZ^*)$	$g^2_{HZZ}g^2_{HZZ}/\Gamma_H$	tbd	–	–
$H\nu_e\bar{\nu}_e$	$\sigma(H\nu_e\bar{\nu}_e) \times \mathrm{BR}(H \to b\bar{b})$	$g^2_{HWW}g^2_{Hbb}/\Gamma_H$	3%†	0.3%	0.2%
$H\nu_e\bar{\nu}_e$	$\sigma(H\nu_e\bar{\nu}_e) \times \mathrm{BR}(H \to c\bar{c})$	$g^2_{HWW}g^2_{Hcc}/\Gamma_H$	–	2.9%	2.7%
$H\nu_e\bar{\nu}_e$	$\sigma(H\nu_e\bar{\nu}_e) \times \mathrm{BR}(H \to gg)$		–	1.8%	1.8%
$H\nu_e\bar{\nu}_e$	$\sigma(H\nu_e\bar{\nu}_e) \times \mathrm{BR}(H \to \tau^+\tau^-)$	$g^2_{HWW}g^2_{H\tau\tau}/\Gamma_H$	–	4.2%	tbd
$H\nu_e\bar{\nu}_e$	$\sigma(H\nu_e\bar{\nu}_e) \times \mathrm{BR}(H \to \mu^+\mu^-)$	$g^2_{HWW}g^2_{H\mu\mu}/\Gamma_H$	–	38%	16%
$H\nu_e\bar{\nu}_e$	$\sigma(H\nu_e\bar{\nu}_e) \times \mathrm{BR}(H \to \gamma\gamma)$		–	15%	tbd
$H\nu_e\bar{\nu}_e$	$\sigma(H\nu_e\bar{\nu}_e) \times \mathrm{BR}(H \to Z\gamma)$		–	42%	tbd
$H\nu_e\bar{\nu}_e$	$\sigma(H\nu_e\bar{\nu}_e) \times \mathrm{BR}(H \to WW^*)$	g^4_{HWW}/Γ_H	tbd	1.4%	0.9%
$H\nu_e\bar{\nu}_e$	$\sigma(H\nu_e\bar{\nu}_e) \times \mathrm{BR}(H \to ZZ^*)$	$g^2_{HWW}g^2_{HZZ}/\Gamma_H$	–	3%†	2%†
Hee	$\sigma(Hee) \times \mathrm{BR}(H \to b\bar{b})$	$g^2_{HZZ}g^2_{Hbb}/\Gamma_H$	–	1%†	0.7%†
$t\bar{t}H$	$\sigma(t\bar{t}H) \times \mathrm{BR}(H \to b\bar{b})$	$g^2_{Ht\bar{t}}g^2_{Hbb}/\Gamma_H$	–	8%	tbd
$HH\nu_e\bar{\nu}_e$	$\sigma(HH\nu_e\bar{\nu}_e)$	g_{HHWW}	–	7%*	3%*
$HH\nu_e\bar{\nu}_e$	$\sigma(HH\nu_e\bar{\nu}_e)$	λ	–	32%	16%
$HH\nu_e\bar{\nu}_e$	with −80% e^- polarisation	λ	–	24%	12%

Results without beam polarisation $\quad$ †: estimated, *: preliminary

Higgs coupling to mass

- Combine results of studied Higgs production and decay channels in global fit → extract couplings and Higgs width
- Fully model independent approach, unique for lepton colliders

Based on results from full Geant4 detector simulations including backgrounds →

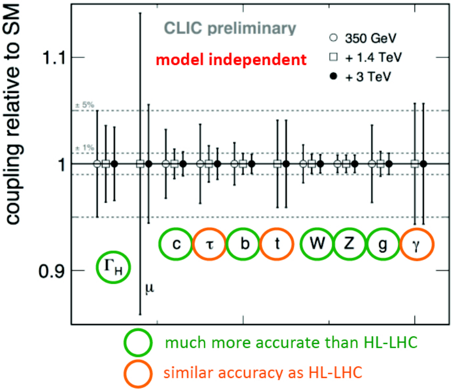

Assuming 80 % electron beam polarisation at 1.4 TeV and 3 TeV

- Paper draft "Higgs Physics at the CLIC Electron-Positron Linear Collider" currently in collaboration review

CLIC physics aims → detector needs

- Momentum resolution
  - Higgs recoil mass, smuon endpoint, Higgs coupling to muons

  → $\sigma_{p_T}/p_T^2 \sim 2\times10^{-5}\mathrm{GeV}^{-1}$
- Jet energy resolution
  - Separation of W/Z/H di-jets

  → $\sigma_E/E \sim 3.5\%$ for jets above 100 GeV
- Impact parameter resolution
  - c/b-tagging, Higgs branching ratios

  → $\sigma_{r\varphi} \sim 5 \oplus 15/(p[\mathrm{GeV}]\sin^{\frac{3}{2}}\theta)\mu m$
- Angular coverage
  - Very forward electron tagging

  → Down to $\theta = 10\,\mathrm{mrad}$
- Requirements from CLIC beam structure and beam-induced backgrounds

Example: H→ $\mu\mu$

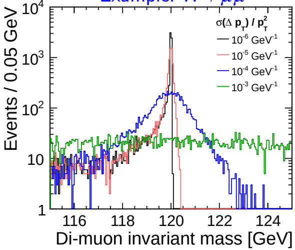

Example: W/Z separation

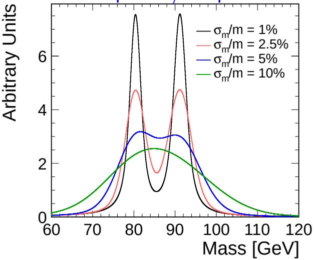

CLIC detector needs: beam-induced backgrounds

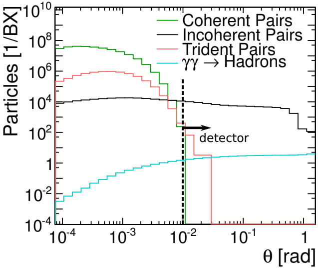

- Small bunch size: $\sigma_{x,y,z} = \{40\,\text{nm}, 1\,\text{nm}, 44\,\mu\text{m}\}$
  $\rightarrow$ strong beam-beam interactions
- Resulting background mostly at low p_T and low θ
- Reject backgrounds using timing and p_T cuts
- Requirement:
  High detector granularity in space and time

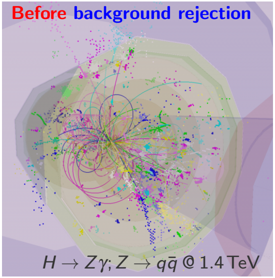

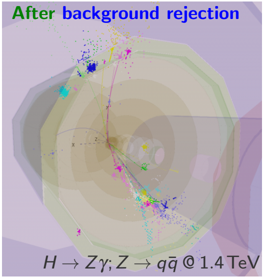

CLIC detector concept

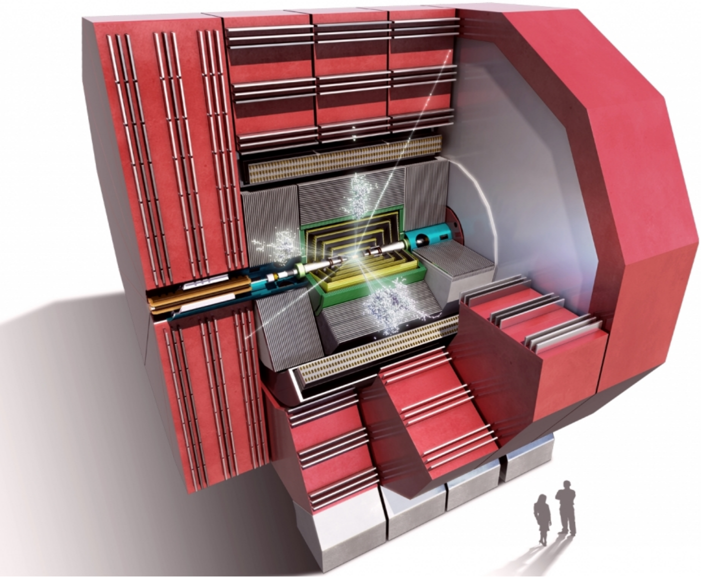

Vertex detector requirements for CLIC

- Single point resolution of $\sigma < 3\,\mu$m
  $\rightarrow$ pixel pitch $\approx 25\,\mu$m, analogue readout

$\rightarrow$ Comprehensive vertex R&D

- Material budget $< 0.2\,\% X_0$ per layer
  $\rightarrow$ $50\,\mu$m sensor+$50\,\mu$m ASIC, low mass support, power pulsing, air cooling
- Time stamping ≤ 10 ns

thin silicon sensor

electronics chip (65 nm)

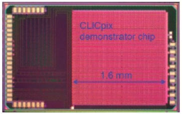

thin electronics + sensor assembly

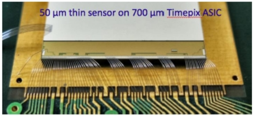

test beam experiments

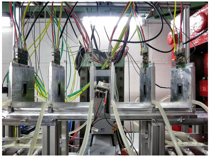

HV-CMOS sensor + CLICpix

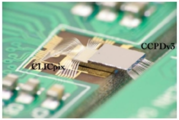

interconnect technology

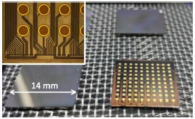

signal simulations

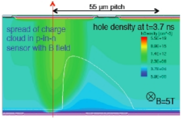

EUTelescope

Device Under Test

power delivery + pulsing

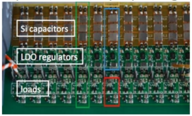

thin supports

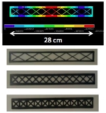

air cooling simulations/tests

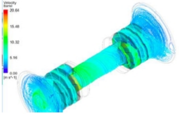

Vertex detector requirements for CLIC

→Vertex and tracking session (Thursday)

- Single point resolution of $\sigma < 3\,\mu$m
  → pixel pitch $\approx$25 μm, analogue readout
- Material budget $< 0.2\,\%X_0$ per layer
  → 50 μm sensor+50 μm ASIC, low mass support, power pulsing, air cooling
- Time stamping $\leq$ 10 ns

→ Comprehensive vertex R&D

thin silicon sensor

electronics chip (65 nm)

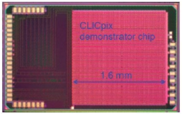

thin electronics + sensor assembly

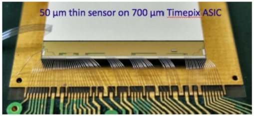

test beam experiments

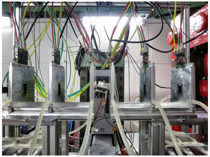

HV-CMOS sensor + CLICpix

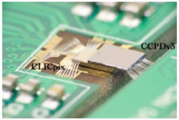

interconnect technology

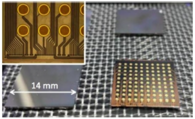

signal simulations

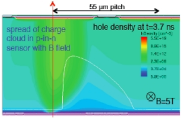

EUTelescope

Device Under Test

power delivery + pulsing

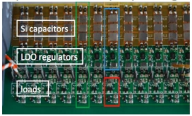

thin supports

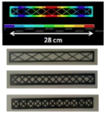

air cooling simulations/tests

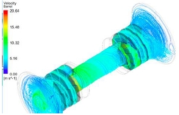

Test beam experiments with Timepix assemblies

- Test beam experiments with Timepix hybrid pixel-detector assemblies
  - Pixel size 55 μm
  - Sensor thickness 50–500 μm

Cluster size versus thickness (55 μm pitch)

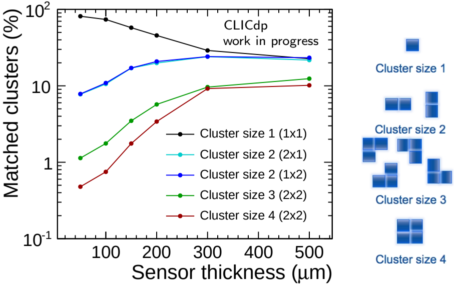

- Charge sharing increases with sensor thickness

Residual for 55 μm pitch size and 50 μm sensor

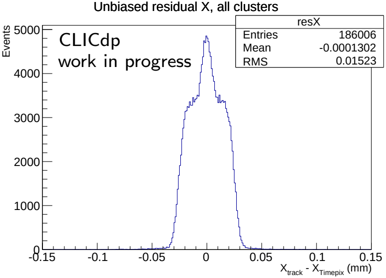

- 1-hit cluster RMS $\sim$ 18 μm
- 2-hit cluster RMS $\sim$ 4.1 μm

- Reduce pixel size ($\rightarrow$25 μm) for higher charge sharing
  $\rightarrow$ improved resolution for the expected 50 μm thickness

Test beam experiments with CLICpix+HV-CMOS

CLICpix+HV-CMOS, 25 μm pitch

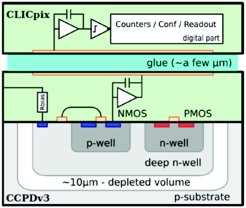

- First proof of principle in a test beam

← Glueing solves limitation of bump bonding at very fine pitch

- Comparison of performance of **1** and **2** sensor amplification stages

Bias voltage scan at low threshold

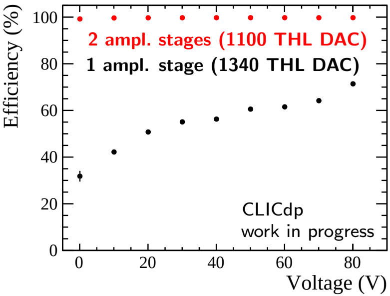

Threshold scan at $V_{bias} = 60\,V$

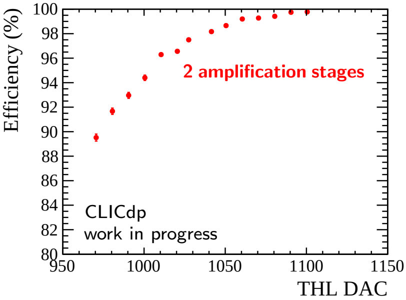

Vertex detector cooling

- Vertex detector with low material budget
  → Power pulsing and air cooling
- Heat load of 50 mW/cm^2 extractable using spiral air flow
  → Test concept in simulations
- Verify simulation results using real size vertex-detector mockup
  - Visual test of air flow using smoke
  - Study spiral air-flow feasibility, temperature and vibrations

Simulation of air flow and heat transport

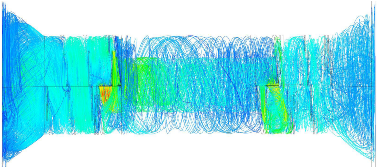

Visual test of spiral air flow

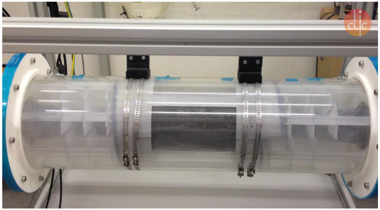

Measurement of velocity and temperature

High-granularity calorimetry: CALICE

Sampling calorimeter

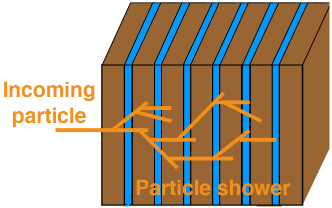

- Neutral particles are invisible in tracking detectors → use calorimeters
- Jet energy resolution goal 3.5% above 100 GeV
  → high-granularity sampling calorimeters
  → readout cell size of few cm^2
- CALICE test beam experiments + analysis:
  - Electromagnetic/Hadronic calorimeters
  - W and Fe as absorbers
  - Analogue and digital readout
    Example: Scintillator tiles+SiPM

CALICE test beam experiments

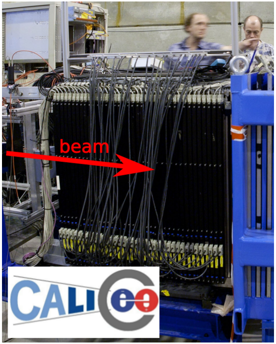

Scintillator tile + SiPM

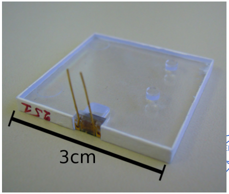

High-granularity calorimetry: CALICE

→Calorimetry session (Tuesday)

Sampling calorimeter

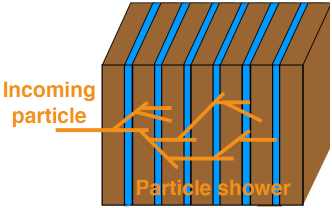

- Neutral particles are invisible in tracking detectors → use calorimeters
- Jet energy resolution goal 3.5% above 100 GeV
  → high-granularity sampling calorimeters
  → readout cell size of few cm^2
- CALICE test beam experiments + analysis:
  - Electromagnetic/Hadronic calorimeters
  - W and Fe as absorbers
  - Analogue and digital readout
    Example: Scintillator tiles+SiPM

CALICE test beam experiments

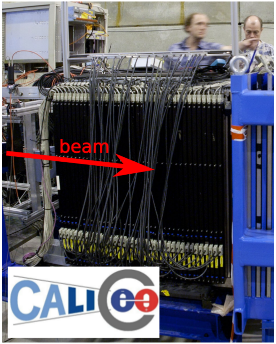

Scintillator tile + SiPM

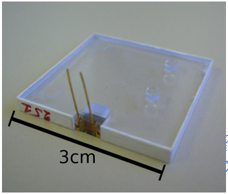

Scintillator and SiPM R&D

- AHCAL analysis→need for deeper understanding
- Dedicated lab for Scintillator and SiPM testing
- Test bench: electron gun, DUT on movable table, trigger scintillators, read-out electronics
- Study uniformity of response, cross-talk, ...

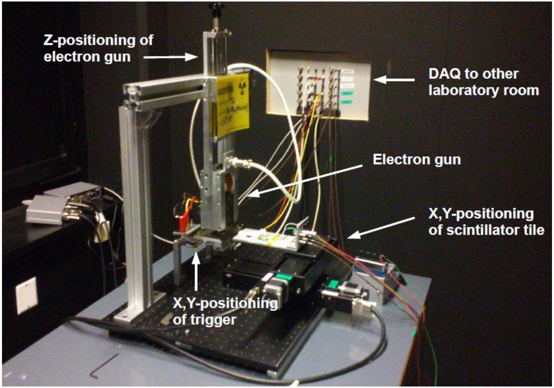

Development of FPGA based DAQ using AGH FE and ADC

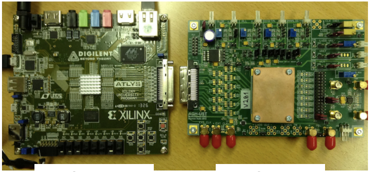

FPGA board ADC board

Calibrated Scint+SiPM response

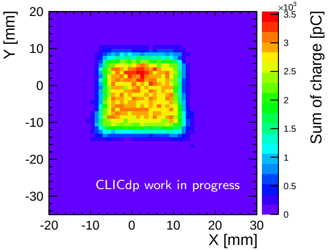

Forward CALorimetry: FCAL

- Very forward e.m. calorimeters (LumiCal + BeamCal)
- Very compact design (sensors, read-out + tungsten plates)

← FPGA based back-end electronics

↙ 4 pairs of front-end ASICs and ADC (read-out for 32 channels)

↗ LumiCal Si sensor (one sector) covered with Kapton fan-out

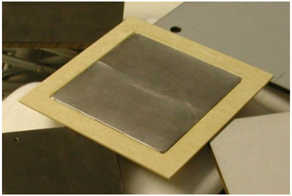

↑ Precision-machined W plates (flatness/roughness$<20/10\mu$m) precision-mounted in permaglass frame

↓ October 2014: first test beam (CERN-PS) with multilayer structure (4 sensor planes; 11 tungsten plates; different configurations)

Forward CALorimetry: FCAL

→Calorimetry session (Tuesday)

- Very forward e.m. calorimeters (LumiCal + BeamCal)
- Very compact design (sensors, read-out + tungsten plates)

↗ LumiCal Si sensor (one sector) covered with Kapton fan-out

← FPGA based back-end electronics

↙ 4 pairs of front-end ASICs and ADC (read-out for 32 channels)

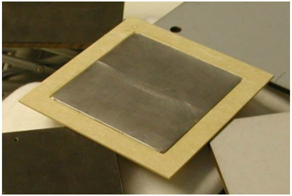

↑ Precision-machined W plates (flatness/roughness$<20/10\mu$m) precision-mounted in permaglass frame

↓ October 2014: first test beam (CERN-PS) with multilayer structure (4 sensor planes; 11 tungsten plates; different configurations)

One CLIC detector model

- Vertex
  - Double layer
  - Inner radius: 31 mm
- Full Silicon tracker
  - Outer radius R: 1.5 m
  - Half length L/2: 2.3 m
  - Single/double layer: Under investigation
- ECAL
  - Silicon and Tungsten
  - 25 layers
- HCAL
  - Scintillator and Steel
  - Cell size: under investigation
  - Acceptance: under investigation
- Magnetic field: 4T
- QD0 and forward region configuration
  - Under investigation
- ...

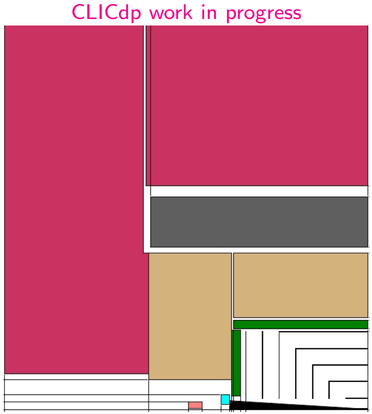

- **Goal:** Finalize CLIC detector model including software and validation by mid 2015

One CLIC detector model

→Detector optimisation session (Wednesday)

→Talk by J. Marshall (Friday)

- Vertex
  - Double layer
  - Inner radius: 31 mm
- Full Silicon tracker
  - Outer radius R: 1.5 m
  - Half length L/2: 2.3 m
  - Single/double layer: Under investigation
- ECAL
  - Silicon and Tungsten
  - 25 layers
- HCAL
  - Scintillator and Steel
  - Cell size: under investigation
  - Acceptance: under investigation
- Magnetic field: 4T
- QD0 and forward region configuration
  - Under investigation
- ...

CLICdp work in progress

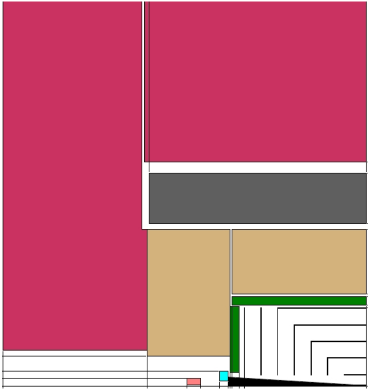

- **Goal:** Finalize CLIC detector model including software and validation by mid 2015

Detector Description for HEP: DD4hep

- Full detector description, one description for all applications
- First version of CLIC simulation model now available in DD4hep
- Validation of simulation and development of reconstruction ongoing
- Synergies with AIDA, ILC, FCC

DD4hep schematic overview

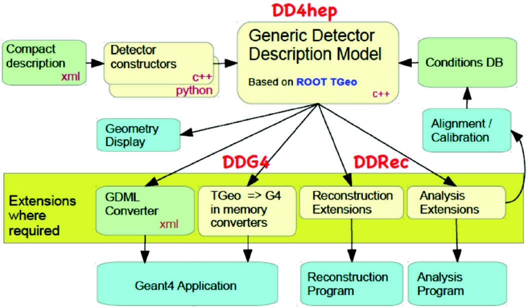

CLIC simulation model in DD4hep

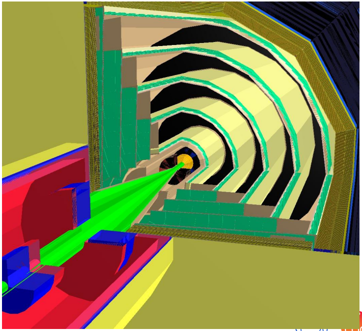

Detector Description for HEP: DD4hep

- Full detector description, one description for all applications
- First version of CLIC simulation model now available in DD4hep
- Validation of simulation and development of reconstruction ongoing
- Synergies with AIDA, ILC, FCC

DD4hep schematic overview

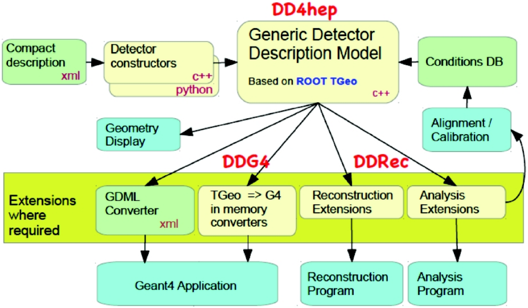

CLIC simulation model in DD4hep

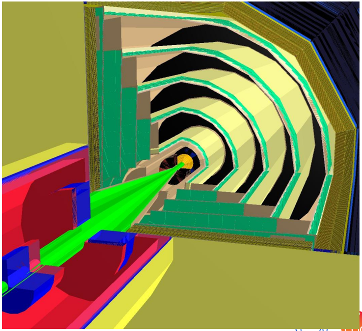

→CLICdp session (Tuesday)

Grid framework ILCDirac

- Analysis and simulations jobs are processed on the grid
- ILCDirac is the grid framework used in CLICdp
- Increasing number of users in LC community
  → ILD plans to move to ILCdirac for future productions

CPU usage by site

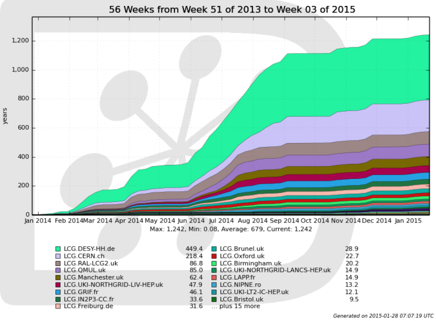

CPU usage by user

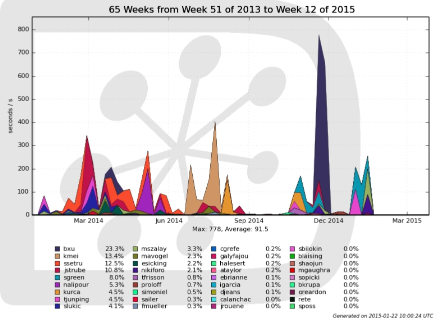

CLICdp Summary

- CLICdp collaboration is very active and it attracts more and more institutes
- Physics benchmark studies show excellent detector performance
- Higgs physics potential of CLIC has been extensively assessed
- Hardware R&D on pixel detectors and calorimeters
- One CLIC detector concept expected for mid 2015
- Software development: detector optimisation, physics benchmark analyses

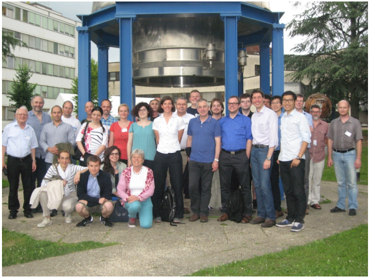

Backup

Compact Linear Collider

CLIC is the only mature option for a future multi-TeV e^+e^--collider

- Gradient of 100 MV/m
- Staged $\sqrt{s}$ up to to 3 TeV
- New: Updating staging scenario
  → Lowest energy stage between 350–500 GeV
  → Trade-off between top and Higgs physics
- High luminosity ($\sim 10^{34}\,\mathrm{cm}^{-2}\mathrm{s}^{-1}$) achievable due to small bunch size

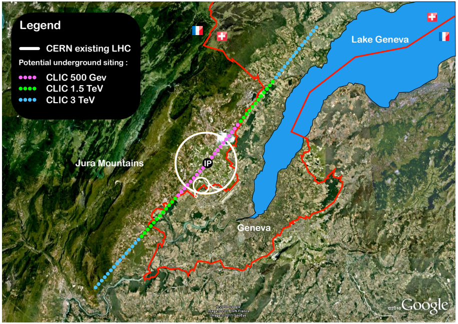

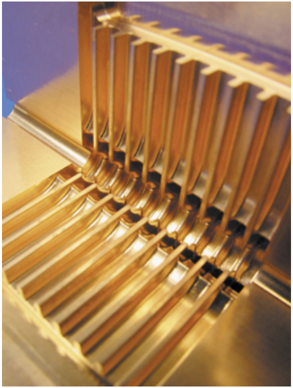

- Prototype of copper accelerating structures for CLIC

Pixel detector simulations

- AllPix (Geant4) simulation of EUTelescope and DUT
- Simulation of Silicon and readout chip
- Overall good agreement between data and simulation, small discrepancies in charge sharing are under investigation

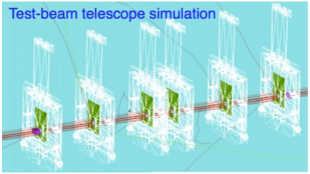

- TCAD simulation of field behaviour at sensor edge
- Goal: improve understanding of active edge sensors needed

AllPix simulation of EUTelecope setup

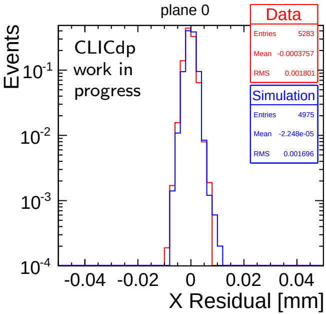

TCAD simulation of field behaviour

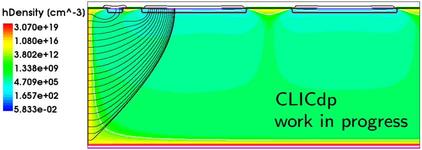

CALICE Tungsten Analogue HCAL

- Analysis of test beam data of highly granular scintillator tungsten HCAL (cell size $3 \times 3\,\text{cm}^2$)
- Electrons and hadrons, 1–300 GeV

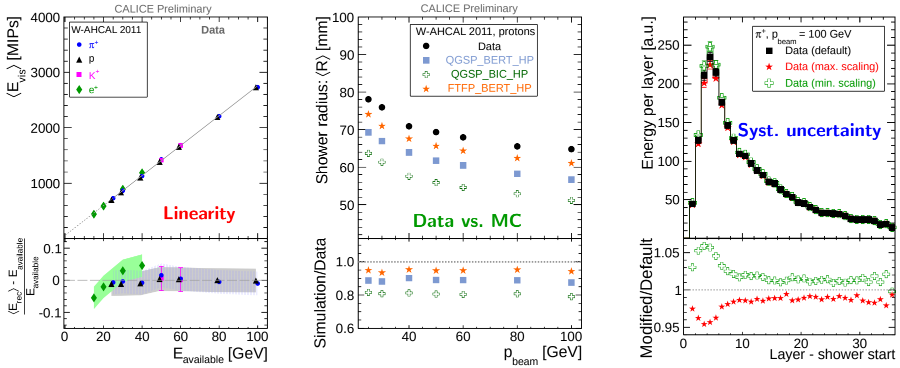

- Study linearity of detector response and energy resolution
  $a_{e^+} = (29.6 \pm 0.5)\%, b_{e^+} = (0.0 \pm 2.1)\%,\ a_{\pi^+} = (61.8 \pm 2.5)\%, b_{\pi^+} = (7.7 \pm 3.0)\%$
- Comparison of Data-Geant4, room for improvements for shower shapes description
- Comprehensive study of all relevant systematic uncertainties

$\rightarrow$ Publication including beam momenta up to 150 GeV in early 2015

CALICE Tungsten Digital HCAL

- Analysis of test beam data of highly granular RPC tungsten HCAL (cell size $1 \times 1\,\mathrm{cm}^2$)
- Electrons and hadrons, 1–300 GeV
- Ongoing study of
  - Data quality
  - Detector calibration: layer and run wise calibration
  - Realistic detector simulation

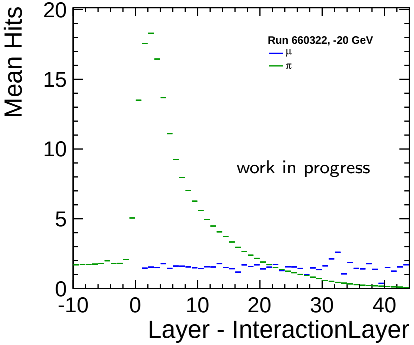

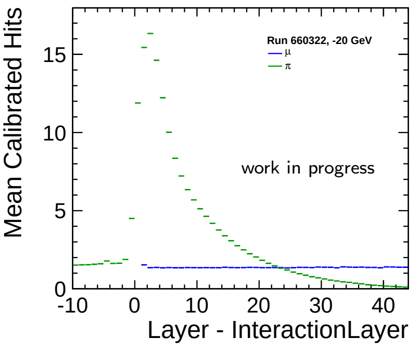

CALICE Tungsten Digital HCAL

- Analysis of test beam data of highly granular RPC tungsten HCAL (cell size $1 \times 1\,\mathrm{cm}^2$)
- Electrons and hadrons, 1–300 GeV
- Ongoing study of
  - Data quality
  - Detector calibration: layer and run wise calibration
  - Realistic detector simulation

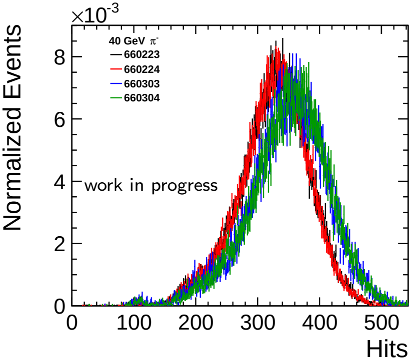

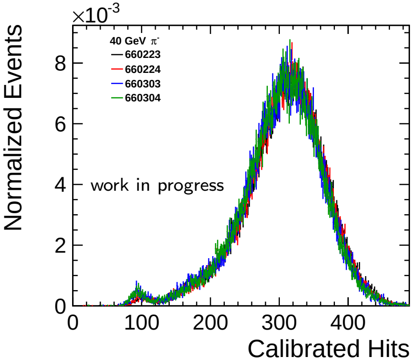

Vertex detector

- Flavor tagging as gauge for detector optimisation
- Note: Tagging performance will also have impact on running time
  1. Single versus double layers → double layers
  2. More realistic material budget → $0.2\% X_0$ per layer
  3. Vary inner radius (connected to choice of B-field) → R=31 mm

1. Single/double layers

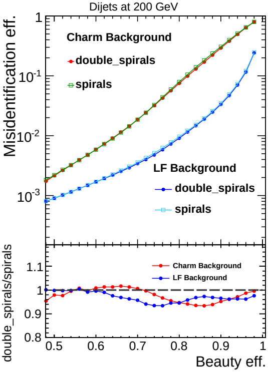

2. $0.1\% X_0 / 0.2\% X_0$

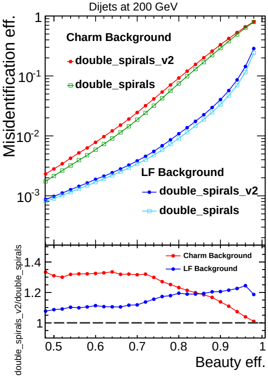

3. Inner radius 27 mm/31 mm

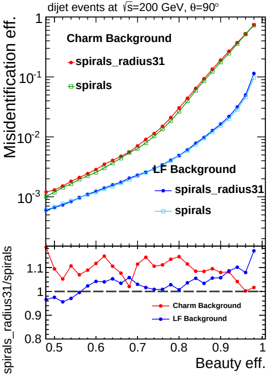

Main tracker and B Field

Gluckstern's formula: $\frac{\sigma(p_T)}{p_T^2} \propto \frac{1}{B \cdot R^2}$

- Improvement with larger tracker size
  - R=1.25 m → 1.5 m
  - L/2=1.6 m → 2.3 m (= +2 disks)
- Worsening with smaller B-field
  - Improved resolution due to enlarged tracker allows for a reduction of B-field
  - Performance degradation 10% per 0.5 T
  - With B=4 T and extended tracker better performance than in CDR

Extended tracker layout

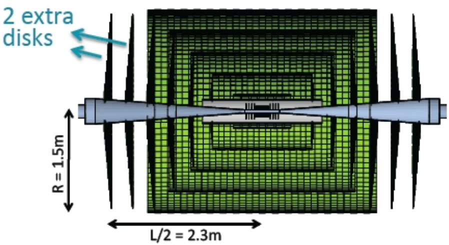

μ momentum resolution at $\theta = 90^\circ$ and 20°

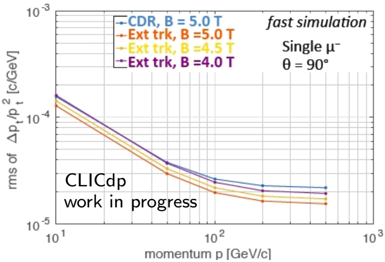

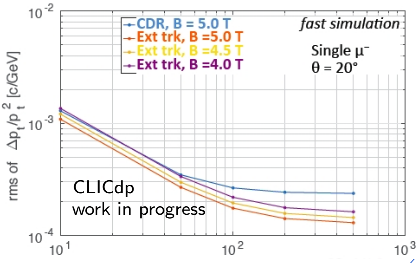

Barrel HCAL: Absorber material

- Comparison of HCAL absorber materials tungsten and steel for $\sim 7.5\,\Lambda_I$
  - W: 75 layers, 10 mm absorber, timing cut 100 ns
  - Fe: 60 layers, 19 mm absorber, timing cut 10 ns
- Compare performance for
  - Single particle reconstruction
  - Jet reconstruction
    $\rightarrow$ Di-jet events $Z \rightarrow qq$
    $\rightarrow$ W/Z separation
- Separation performance similar for tungsten and steel
- Steel cheaper, easier to process

$\Rightarrow$ Use steel as absorber material for barrel HCAL

$WW \rightarrow \nu l u d$, $ZZ \rightarrow \nu\nu d d$